

SANDIA REPORT

SAND96-1992 • UC-1211
Unlimited Release
Printed August 1996

A Generalized Fitting Technique for the LIFE2 Fatigue Analysis Code

RECEIVED
SEP 18 1996
OSTI

Herbert J. Sutherland
Wind Energy Research Department
Sandia National Laboratories
Albuquerque, NM 87185

Tracy Wilson
New Mexico Engineering Research Institute
University of New Mexico
Albuquerque, NM 87106

Prepared by
Sandia National Laboratories
Albuquerque, New Mexico 87185 and Livermore, California 94550
for the United States Department of Energy
under Contract DE-AC04-94AL85000

Approved for public release; distribution is unlimited.

Issued by Sandia National Laboratories, operated for the United States Department of Energy by Sandia Corporation.

NOTICE: This report was prepared as an account of work sponsored by an agency of the United States Government. Neither the United States Government nor any agency thereof, nor any of their employees, nor any of their contractors, subcontractors, or their employees, makes any warranty, express or implied, or assumes any legal liability or responsibility for the accuracy, completeness, or usefulness of any information, apparatus, product, or process disclosed, or represents that its use would not infringe privately owned rights. Reference herein to any specific commercial product, process, or service by trade name, trademark, manufacturer, or otherwise, does not necessarily constitute or imply its endorsement, recommendation, or favoring by the United States Government, any agency thereof or any of their contractors or subcontractors. The views and opinions expressed herein do not necessarily state or reflect those of the United States Government, any agency thereof or any of their contractors.

Printed in the United States of America. This report has been reproduced directly from the best available copy.

Available to DOE and DOE contractors from
Office of Scientific and Technical Information
PO Box 62
Oak Ridge, TN 37831

Prices available from (615) 576-8401, FTS 626-8401

Available to the public from
National Technical Information Service
US Department of Commerce
5285 Port Royal Rd
Springfield, VA 22161

NTIS price codes
Printed copy: A03
Microfiche copy: A01

DISCLAIMER

**Portions of this document may be illegible
in electronic image products. Images are
produced from the best available original
document.**

SAND96-1992
Unlimited Distribution
Printed August, 1996

A GENERALIZED CURVE FITTING TECHNIQUE FOR THE LIFE2 FATIGUE ANALYSIS CODE

by

HERBERT J. SUTHERLAND
Wind Energy Research Department
Sandia National Laboratories
Albuquerque, NM 87185

and

TRACY WILSON
New Mexico Engineering Research Institute
University of New Mexico
Albuquerque, NM 87106

ABSTRACT

The fatigue analysis of wind turbine components typically depends on the use of representative samples of stress histories to predict the fatigue load spectrum on the turbine during its lifetime. A generalized fitting technique, developed by Winterstein and Lange [1,2], has been shown to be particularly useful for matching the body of the distribution of fatigue stress cycles on a turbine component and for extrapolating the tail of the distribution to remove the artificial truncation of large amplitude cycles that is inherent in finite data samples. The numerical algorithms developed by Winterstein and Lange, with a series of pre- and post-processing algorithms, have been incorporated into the LIFE2 fatigue analysis code for wind turbines. This report describes the algorithms incorporated into the code and their numerical implementation. Example problems are used to illustrate typical inputs and outputs.

ACKNOWLEDGMENTS

The generalized Weibull fitting technique used here and its numerical algorithm were developed by Steven Winterstein and Clifford Lange, Department of Civil Engineering, Stanford University. The authors thank them for the excellent numerical subroutine used here. Also, detailed discussions with them and with Paul Veers have expedited the incorporation of the subroutine into the LIFE2 code and have greatly enhanced the utility of this option.

TABLE OF CONTENTS

Acknowledgments	iv
Table of Contents	v
List of Figures	vi
Introduction	1
Generalized Fitting Algorithm	2
Implementation	2
Typical Data	3
Preprocessing Algorithms	7
Parent Distribution	7
Lower Bound	7
Truncation	8
The Fitting Algorithms	10
Post-Processing Algorithms	10
Low Stress Cycles	10
Total Number of Cycles	11
Binned Data	11
Mean Stress Level	11
Summary	11
Another Example	12
Concluding Remarks	15
Bibliography	16
Appendix A: Example Session with Typical Results	18
Documenting Units	18
Operator Inputs	18
Access	18
Curve Fitting from the Limited Time Data Menu	20
Appendix B: Plotting the Results	24

LIST OF FIGURES

Fig. 1.	The NPS Turbine	3
Fig. 2.	Typical Stress Cycle Matrix for the 100-kW NPS Wind Turbine, Edgewise Bending Moment	4
Fig. 3.	Typical Stress Cycle Matrix for the 100-kW NPS Wind Turbine, Flapwise Bending Moment	4
Fig. 4	Typical Alternating Stress Cycle Counts for the 100-kW NPS Wind Turbine, Edgewise Bending Moment	5
Fig. 5	Typical Alternating Stress Cycle Counts for the 100-kW NPS Wind Turbine, Flatwise Bending Moment	5
Fig. 6	Generalized Weibull Plot of the Alternating Stress Cycle Counts for the 100-kW NPS Wind Turbine, Edgewise Bending Moment	6
Fig. 7	Generalized Weibull Plot of the Alternating Stress Cycle Counts for the 100-kW NPS Wind Turbine, Edgewise Bending Moment	6
Fig. 8.	Curve Fit to the Flatwise Bending Moment for the 100-kW NPS Wind Turbine	7
Fig. 9.	Generalized Weibull Plot of the Curve Fit to the Flatwise Bending Moment for the 100-kW NPS Wind Turbine	8
Fig. 10.	Curve Fit to the Edgewise Bending Moment for the 100-kW NPS Wind Turbine	9
Fig. 11.	Generalized Weibull Plot of the Curve Fit to the Edgewise Bending Moment for the 100-kW NPS Wind Turbine	9
Fig. 12.	Generalized Weibull Curve Fit to the Edgewise Bending Moment for the 100-kW NPS Wind Turbine	10
Fig. 13.	Generalized Curve Fit to the Edgewise Bending Moment for the 100-kW NPS Wind Turbine	11
Fig. 14.	The Sandia 34-m Test Bed Turbine	12
Fig. 15.	Comparison of Rainflow Counted Stress Cycles and the Generalized Weibull Fit for the Sandia 34-m VAWT	12
Fig. 16.	Generalized Weibull Plot of Rainflow Counted Stress Cycles and the Generalized Weibull Fit for the Sandia 34-m VAWT	13
Fig. 17.	Comparison of the Frequency Synthesized Stress Cycle Distribution to the Rainflow Counted Stress Cycles and the Generalized Weibull Fit for the Sandia 34-m VAWT	14

Fig. 18. Generalized Weibull Plot of the Frequency Synthesized Stress Cycle Distribution to the Rainflow Counted Stress Cycles and the Generalized Weibull Fit for the Sandia 34-m VAWT	14
Fig. 19. Generalized Weibull Plot of the Frequency Synthesized Stress Cycle Distributions for the Sandia 34-m VAWT	15
Fig. 20. Screen Display for the Generalized Weibull Fit of the 9 to 11 m/s Interval in the Operational Stresses Calculational File	26

INTRODUCTION

The analysis of component fatigue lifetime for a wind energy conversion system (WECS) requires that the component load spectrum be formulated in terms of stress cycles. Typically, these stress cycles are obtained from time series data using a cycle identification scheme such as the "rainflow" counting algorithm. As discussed by many authors [e.g., see Ref. 3], the matrix or matrices of cycle counts that describe the stresses on a turbine are constructed from relatively short, representative samples of time series data. The ability to correctly represent the long-term behavior of the distribution of stress cycles from these representative samples is critical to the analysis of service lifetimes.

Several techniques are currently used to convert representative samples to the lifetime cyclic loads on the turbine. Many designers simply scale the sample loads with time. They note that these limited time measurements or simulations define the main body of the distribution, and assume that they capture all of the necessary loads on the turbine to define its service lifetime. Other designers note that the infrequent occurrences of high-stress events contained in the "tail of the distribution" are affected by the specific data set, and that the distribution tails fill in as more and more data are added to the record. They note that the existence of a "high stress tail" on the distribution has significant influence on the predicted service lifetime of the turbine, and they believe that it must be well defined for an accurate fatigue analysis of a wind turbine. The latter group of designers typically extrapolate from the body of the cycle count distribution into this tail region.

Winterstein and Lange [1] and Winterstein, Lange and Kumar [2] recently developed a set of fitting algorithms that is particularly useful for matching the body of the distribution of fatigue stress cycles on a turbine component. Their technique optimally retains the statistical information of the high-level response data by distorting a parent distribution to fit the first four statistical moments of the data. Importantly, this enables the technique to distort the parent distribution when the data indicate that tail behavior differs from the parent distribution. Three parent distributions are currently available in their fitting algorithms: the Gaussian, the Weibull and the Gumbel distributions.

The Weibull distribution is of particular importance to wind turbine applications because it contains, as special cases, both the exponential and Rayleigh distributions, i.e., the two primary classes of distributions that have been applied to wind turbine cyclic loads data in the past [4,5,6]. Moreover, Winterstein and Lange [1] and Sutherland and Veers [7] have demonstrated that the four-moment Weibull distribution effectively matches wind turbine field data.

This "generalized fitting technique" is now incorporated into the LIFE2 fatigue/fracture analysis code for wind turbines [8]. In this paper, we provide an overview of the fitting algorithms and describe the pre- and post-count algorithms developed to permit their use in the LIFE2 code [9,10]. Complete descriptions of the algorithms and the numerical techniques implemented into the LIFE2 code are contained in Refs. 1 and 2. After a brief overview of these algorithms, typical case studies are used to illustrate the use of the

technique for the cyclic loads on various turbine components. Appendix A is used to illustrate the typical inputs and outputs for the LIFE2 code for one of the examples.

GENERALIZED FITTING ALGORITHM

Typically, the tails of distributions that are found in nature are difficult to infer from the bodies of the distributions, because the tails are often found to differ even when the bodies are similar. The differences are due to behavioral changes that occur when the most severe environments are encountered (e.g., due to nonlinearities, or the initiation of a different mode of response). This causes a skewing, or distortion of the tail from what might be found in a standard distribution model.

Winterstein and Lange [1,2] have introduced a technique that optimally retains the statistical information of the high-level response data. Their generalized fitting technique distorts one of three parent distributions to fit the first *four* statistical moments of the data. Most distribution models use only the first *two* moments. Fitting to the higher moments¹ of the distribution enhances the fit to the largest values in the data. Thus, this fitting technique distorts the parent distribution when the data indicate that tail behavior differs from the parent distribution. The spread of the distribution is particularly important in fatigue analyses.

For wind turbine blade applications, the extrapolation of representative data samples to lifetime cyclic loads has emphasized exponential [4] or Rayleigh [5] distributions. In fact, both the exponential and Rayleigh are just special cases of the more general Weibull distribution. Weibull distributions can model a wide range of behaviors with two parameters to describe the central tendency of the distribution (i.e., the body of the distribution) and the spread of the distribution (i.e., the tail of the distribution). With its versatility and the previous emphasis that has been placed on its use, a generalized Weibull fit will be used exclusively in the examples presented here. However, we should note that the Gaussian and the Gumbel distribution are also available in the LIFE2 code for fitting distributions that do not fall within the typical Weibull parent distribution.

IMPLEMENTATION

The LIFE2 computer code is a fatigue/fracture analysis code specifically designed for the analysis of wind turbine components [8, 9, and 10]. It is a PC-compatible FORTRAN code that is written in a top-down modular format with a user friendly, interactive interface. In this numerical formulation, an "S-n" fatigue analysis is used to describe the initiation, growth and coalescence of micro-cracks into macro-cracks. A linear, "da/dn" fracture analysis is used to describe the growth of a macro-crack.

¹The *i*th moment of a distribution equals the average value of the difference between each value and the mean value of the distribution raised to the *i*th power.

In the LIFE2 formulation, the cyclic stresses imposed on the turbine component are characterized by a series of cycle count matrices. Each matrix describes the stress cycles imposed upon the turbine during one phase of its operation. In general, the cycle count matrices are a two-dimensional matrix of cycle counts. Within each matrix, each stress cycle is characterized by its mean and by its alternating component (either range or amplitude). The cycle count matrices are divided into three groups by the LIFE2 code. The first set describes the stresses on the turbine during normal operation, the second describes transient events (as starting and stopping the turbine), and the third describes wind loads on the turbine when the turbine is not in operation. The fitting algorithm may be used to fit any of the cycle count matrices used by the code to compute service lifetimes.

The algorithms described in this report *only fit the alternating stress component* of the cycle count matrix. The dependence of the cycle count matrix on the mean stress is removed by summing the cycle counts that are characterized by a single alternating stress bin over all means; i.e., if the initial distribution of cycle counts is given by $N[(\sigma_a)_i, (\sigma_m)_j]$, where N is the number of cycle counts in each bin of an I by J matrix, $(\sigma_a)_i$ characterizes the i^{th} alternating component bin and $(\sigma_m)_j$ characterizes the j^{th} mean component bin, then the distribution of the alternating component $\bar{N}[(\sigma_a)_i]$ is given by:

$$\bar{N}[(\sigma_a)_i] = \sum_{j=1}^J N[(\sigma_a)_i, (\sigma_m)_j] \quad [1]$$

This distribution is assumed to have a constant mean stress equal to average mean stress of the original distribution. Thus, the resulting one-dimension vector (matrix) characterizes each stress cycle only by its alternating component.

Appendix A provides a detailed description of the "Example Session" that was used to curve fit the edgewise data analyzed in this section of the paper.

Typical Data

To facilitate this discussion, cycle count matrices from the NPS 100-kW horizontal axis wind turbine will be used in this description of the LIFE2 algorithms. This data set was collected under the auspices of the NREL Cooperative Research Program on the NPS 100-kW turbines in Altamont Pass, California [11]. The NPS turbine is a two-bladed, upwind, teetering hub design utilizing full-span hydraulic passive pitch control, see Fig. 1. A

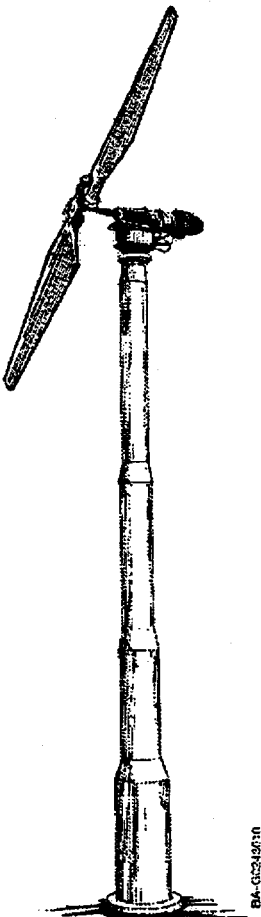


Fig. 1. The NPS Turbine.

plot of a typical operational cyclic stress matrix for the edgewise blade stresses is shown in Figure 2. A plot of the flapwise blade stresses is shown in Figure 3 (These figure were created with the plotting package that is available in the LIFE2 package, see Appendix B). Typical alternating stress cycle count plots for the flapwise and edgewise loads are shown in Figures 4 and 5, respectively. In the "generalized Weibull plots" of these data, see Figures 6 and 7, the cumulative density function (CDF) for the distribution is plotted against the log of the stress range. In this form, the vertical scale of the plot has been distorted in such a way that any Weibull distribution will plot as a straight line [3].

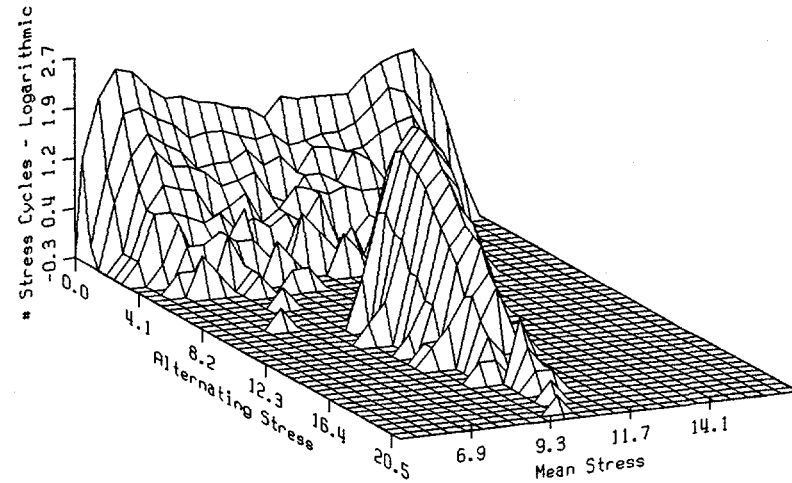


Figure 2. Typical Stress Cycle Matrix for the 100-kW NPS Wind Turbine, Edgewise Bending Moment.

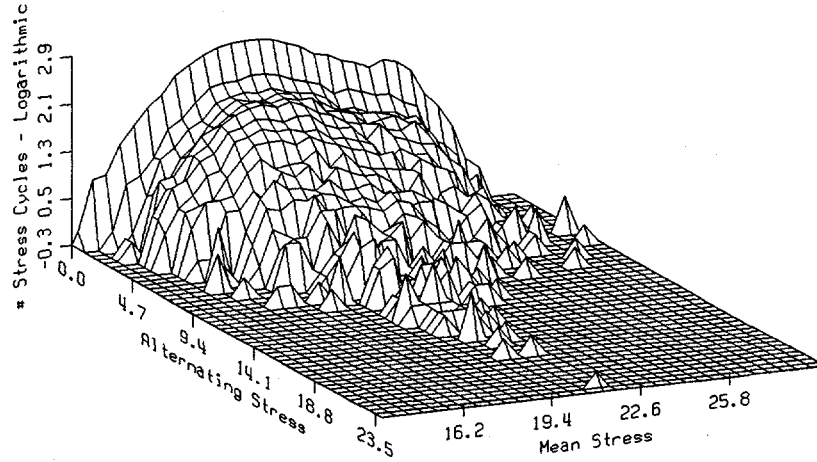


Figure 3. Typical Stress Cycle Matrix for the 100-kW NPS Wind Turbine, Flatwise Bending Moment.

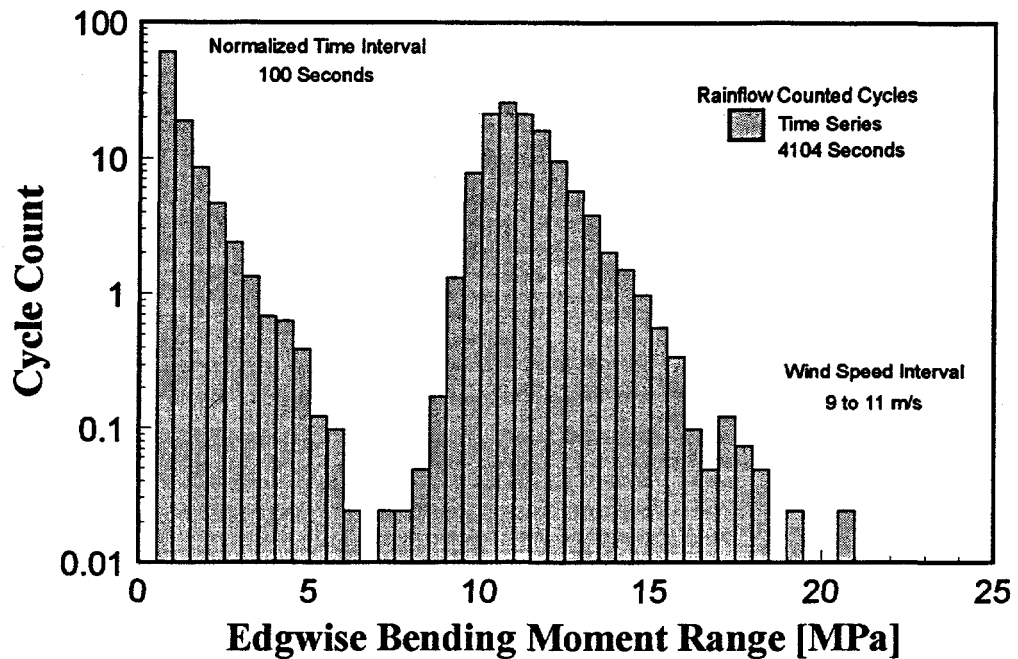


Figure 4. Typical Alternating Stress Cycle Counts for the 100-kW NPS Wind Turbine, Edgewise Bending Moment.

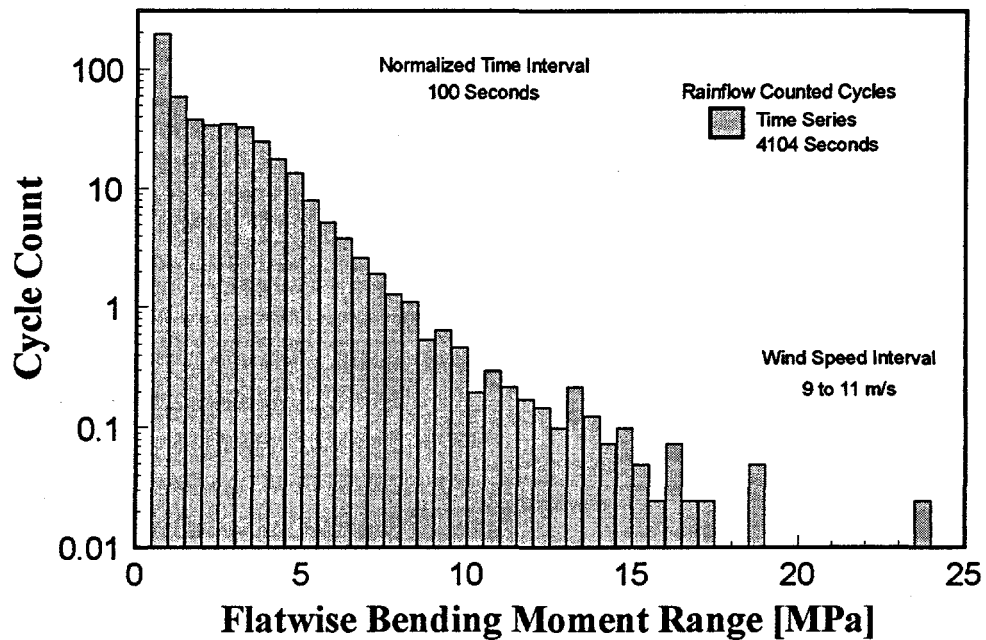


Figure 5. Typical Alternating Stress Cycle Counts for the 100-kW NPS Wind Turbine, Flatwise Bending Moment.

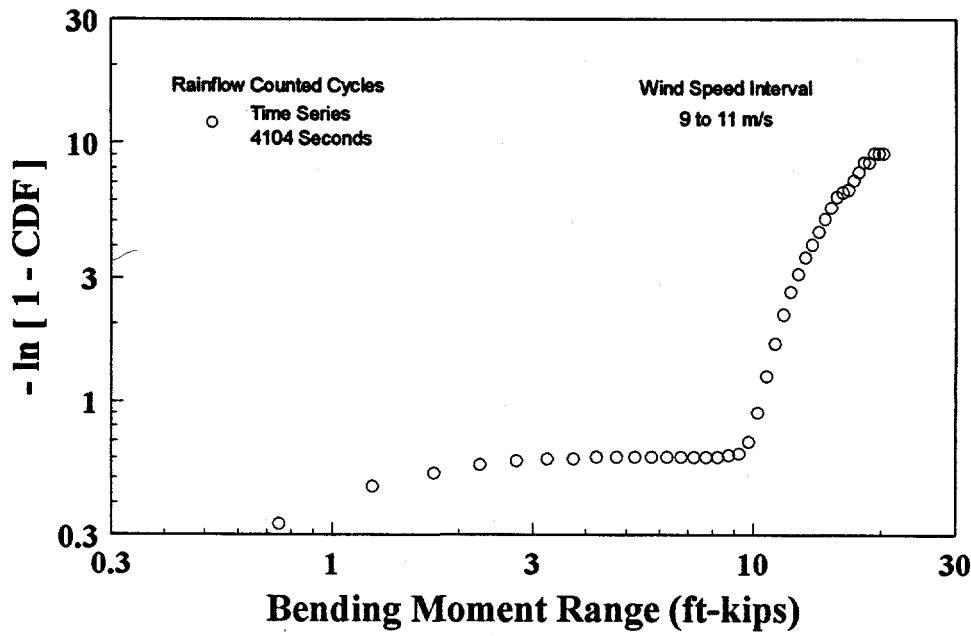


Figure 6. Generalized Weibull Plot of the Alternating Stress Cycle Counts for the 100-kW NPS Wind Turbine, Edgewise Bending Moment.

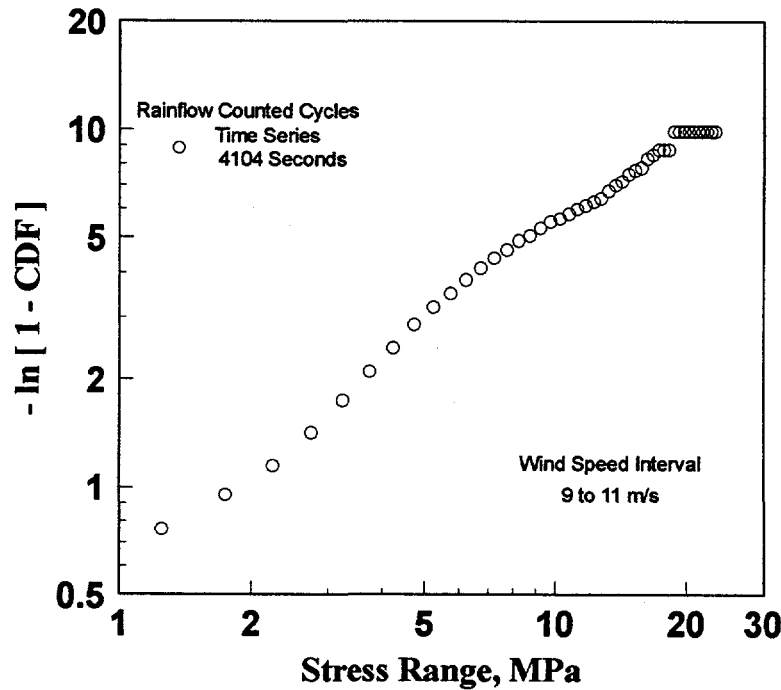


Figure 7. Generalized Weibull Plot of the Alternating Stress Cycle Counts for the 100-kW NPS Wind Turbine, Flapwise Bending Moment.

Preprocessing Algorithms

For the purposes of this discussion, we will assume that the cycle count matrices have been generated previously. These matrices may come from any source, e.g. rainflow counted time series data or frequency synthesized data, as long as they are in the standard LIFE2 file format for the cycle count matrices [9].

The fitting process starts in the LIFE2 code by leading the analyst through a series of menus to chose the cycle count matrix to be analyzed (see Appendix A). Once the matrix has been chosen, the analyst may display a graph of the alternating stress components from that matrix to aid in the selection of the processing parameters.

For this example, we will use the edgewise and the flapwise data described above.

Parent Distribution: Once the matrix for analysis is chosen, the analyst is asked to choose the parent distribution for the fitting process. One of three choices for the parent distribution is permitted: Gaussian, Weibull or Gumbel. As noted above, a Weibull parent distribution will be used exclusively in the examples presented here.

Lower Bound: The analyst is then asked to choose a lower bound for the fit. The lower bound for the curve fit may be chosen anywhere in the distribution. For a typical single mode distribution of stress cycles, see the flapwise data shown in Figures 3, 5 and 7; the lower bound is typically chosen to avoid the large number of cycle counts at the relatively low stress levels. Sensitivity studies conducted by the authors indicate that the lower bound chosen for this case does not significantly change the fit. For these data, a lower bound of 3 MPa was chosen by the authors. The curve fit to these data is shown in Figures 8 and 9.

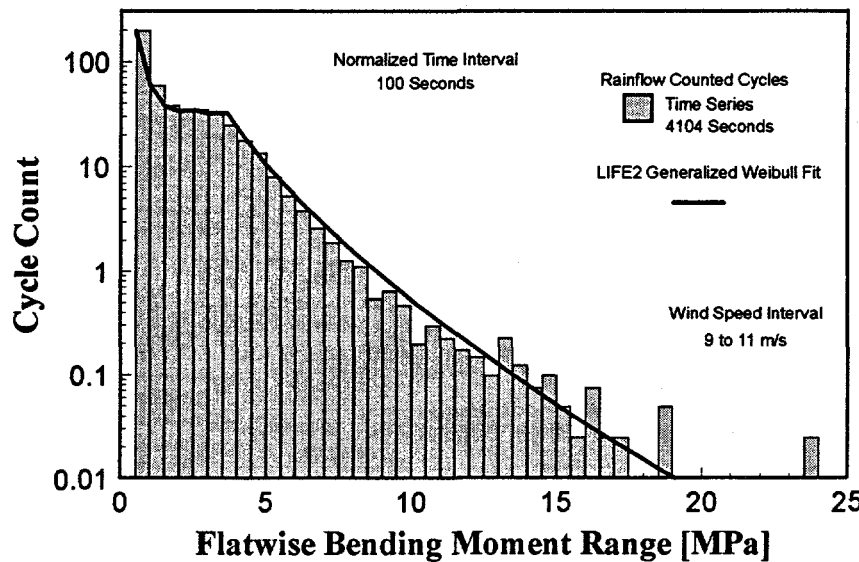


Figure 8. Curve Fit to the Flatwise Bending Moment for the 100-kW NPS Wind Turbine.

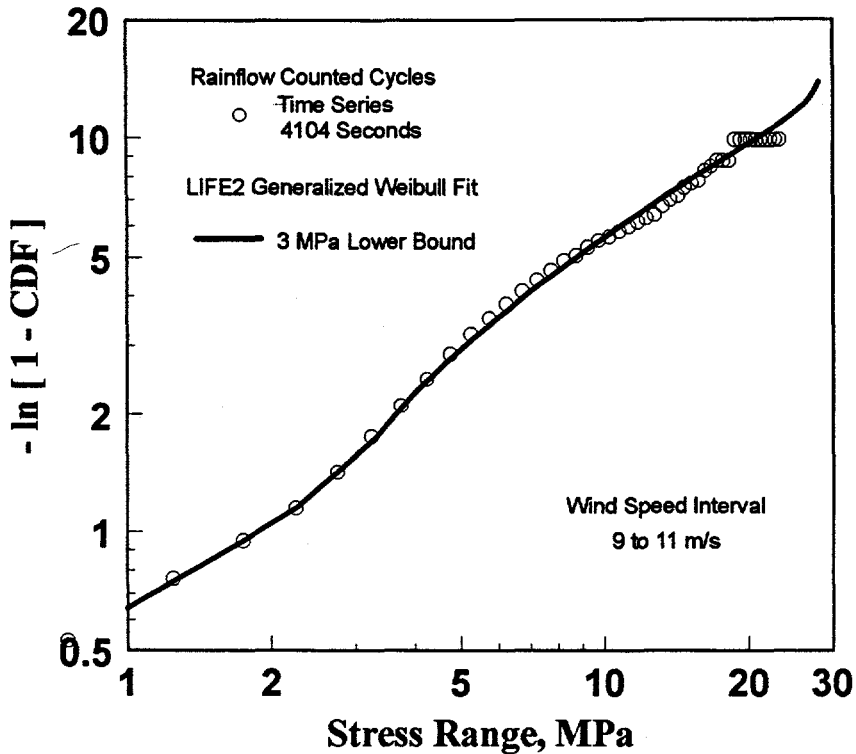


Figure 9. Generalized Weibull Plot of the Curve Fit to the Flatwise Bending Moment for the 100-kW NPS Wind Turbine

When the distribution of stress cycles is bi-modal, as shown in Figure 4, the lower bound becomes very important. The algorithm used here will fit only a single mode of the distribution. In this case, the lower bound should be chosen at or above 8 MPa. The consequences of choosing a smaller lower bound are shown in Figures 10 and 11, where the curve fitting algorithm has tried to fit both modes, and does not fit either one very well. Also shown in the figure is the curve fit to the data above 8 MPa.

Truncation: As noted in Sutherland and Butterfield [3], designers use various techniques to extrapolate the high stress tail of the cycle count distribution. While some designers use the entire extrapolated distribution of load cycles, others question the magnitude of the loads predicted by extrapolation techniques. They feel that the extraordinarily high loads predicted by these techniques have no basis in fact. As this debate began relatively recently, its outcome remains in question. To allow for either viewpoint, the analyst is asked to input a value above which this extrapolation is truncated (this truncation factor as a multiple of the RMS of the distribution being fit). By choosing a large value, the distribution will be truncated at a level where the damage is negligible. The analyst may choose to truncate the distribution at any other level considered prudent. The damage density plots available in the LIFE2 code may be used to determine the importance of the truncation [8, 9].

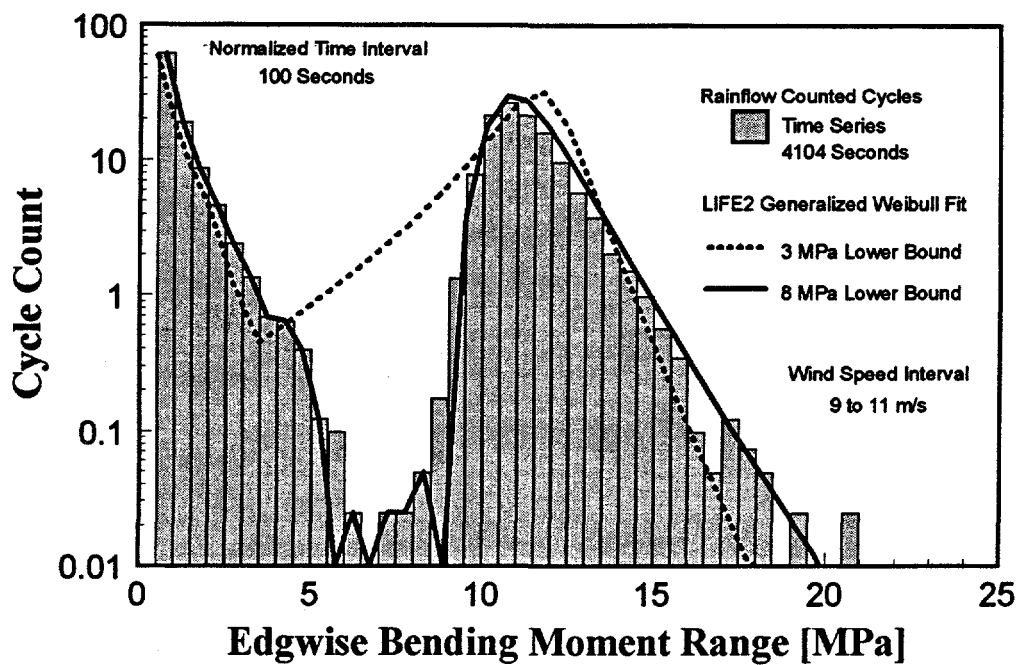


Figure 10. Curve Fit to the Edgewise Bending Moment for the 100-kW NPS Wind Turbine.

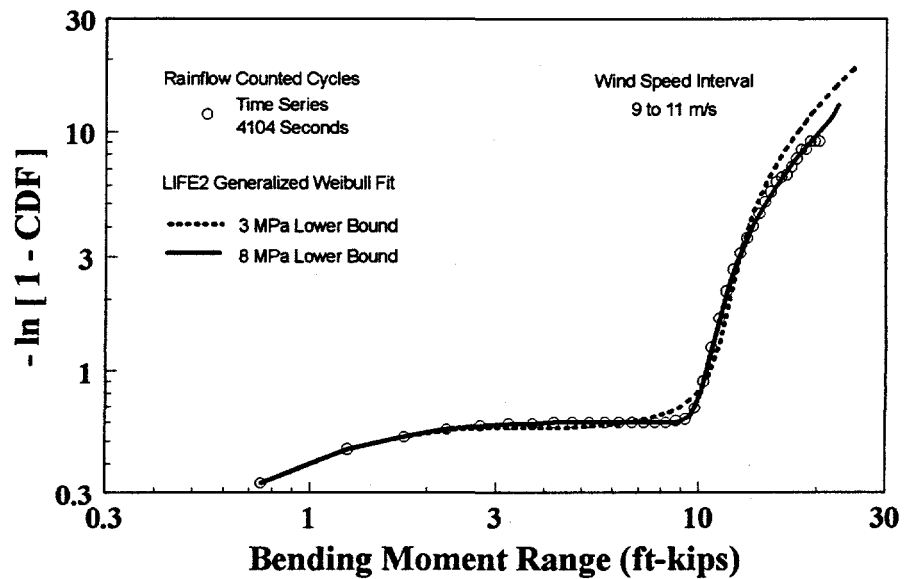


Figure 11. Generalized Weibull Plot of the Curve Fit to the Edgewise Bending Moment for the 100-kW NPS Wind Turbine

The Fitting Algorithm

Based on the parameters supplied above, the generalized fitting technique is applied to the data in the chosen cycle count matrix. To incorporate this algorithm into the LIFE2 code required that the original numerical algorithm developed by Winterstein and Lange [1] be modified to accept binned data.

The original input to the Winterstein and Lange algorithms requires that each stress cycle be characterized by its magnitude (range or amplitude). As the data in the cycle count matrices have been "binned," the exact magnitude of each cycle is not retained; rather, its magnitude has been bounded within the range of its bin. For the LIFE2 analysis, the magnitude of each stress cycle is assumed to be at *the average (the middle) of its respective bin*. Each cycle in each bin is input into the Winterstein and Lange algorithms. These algorithms return the CDF for the fitted distribution. This CDF must be processed before it can be used in the LIFE2 analysis.

Post-Processing Algorithms

The final algorithms in the fitting routine for the LIFE2 code replace the original distribution of cycle counts with the fitted distribution.

Low Stress Cycles: In the technique used here, all stress cycles below the lower bound that have been input by the operator (see above), are left unchanged by the fitting process. As shown graphically in the comparison of Figures 2, 3, 12 and 13 both the mean stress values and the alternating stress value are maintained. Typically these cycles are not important in the fatigue calculation. We have chosen to leave them in the matrix to ensure that their damage contribution is not overlooked by the analysis. Keeping them does not significantly increase computation times, although it does slightly decrease the resolution in the tail of the distribution.

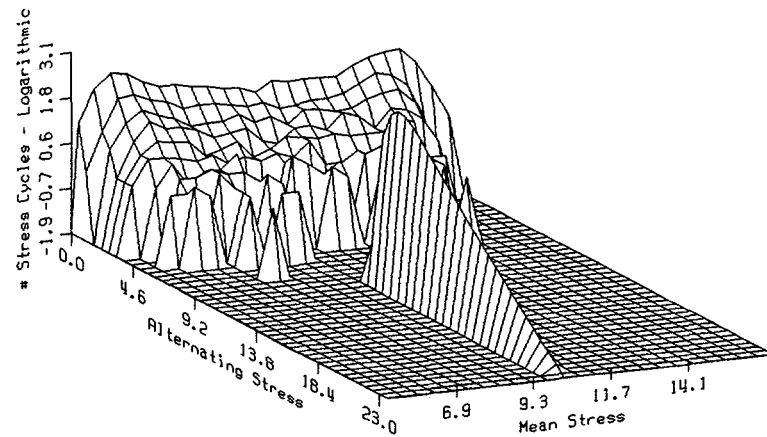


Fig. 12. Generalized Weibull Curve Fit to the Edgewise Bending Moment for the 100-kW NPS Wind Turbine.

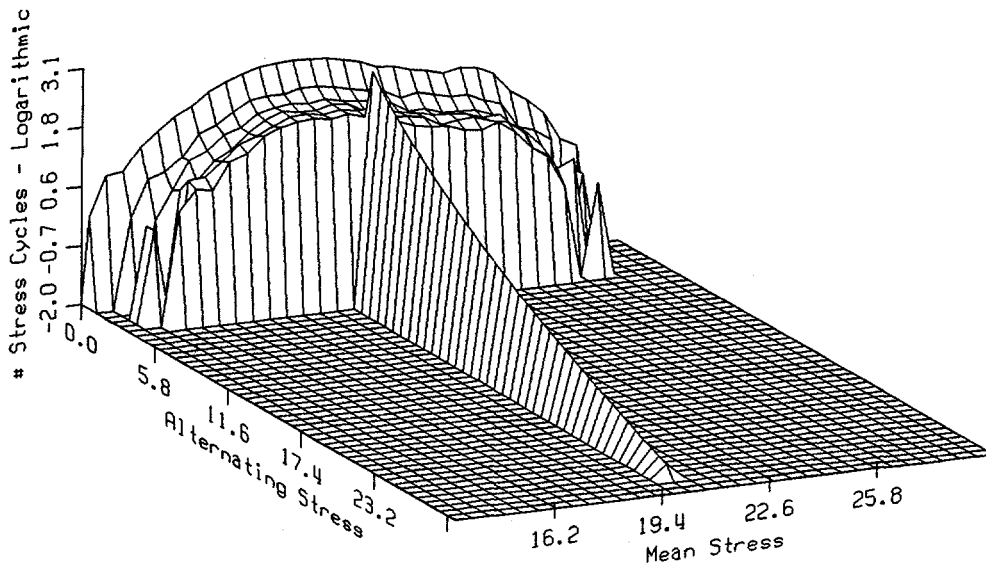


Fig. 13. Generalized Weibull Curve Fit to the Flapwise Bending Moment for the 100-kW NPS Wind Turbine.

Total Number of Cycles: The CDF returned by the fitting algorithms is a normalized fit that must be converted to actual cycle counts before it can be used by the LIFE2 code. For this conversion, the LIFE2 code automatically determines the total number of stress cycles above the “lower bound” before the fitting procedure is initiated. This total number of stress cycles, N_{cycle} , is assumed to remain unchanged by the fitting process. Thus, we have assumed that *total number of cycles before and after the fit remains constant*.

Binned Data: As noted above, the LIFE2 code uses binned data in its analysis procedure. To convert the CDF and N_{cycle} to binned cycle counts, the LIFE2 code automatically sets up a uniform series of bins based on the lower bound input parameter and the truncation parameter. If the i^{th} bin has an upper bound stress of $(\sigma_U)_i$, and a lower bound of $(\sigma_l)_i$, which is equal to $(\sigma_U)_{i-1}$, then the number of cycle counts n_i equals:

$$n_i = N_{cycle} \{ CDF [(\sigma_U)_i] - CDF [(\sigma_U)_{i-1}] \} \quad [2]$$

Mean Stress Level: As the fitting technique does not maintain the distribution of stress cycles with mean stress, the algorithm computes the average mean stress of all of the cycles above the lower bound. All cycle counts contained in the curve fit are taken to be at this average mean stress value, see Figures 12 and 13.

Summary: The post-processing algorithms are executed by the code without intervention from the analyst. Once completed, the analyst may then plot the new

distribution of cycle counts, see Appendix B, process another matrix with the fitting technique, or continue other operations with the code.

Another Example

The Sandia 34-meter diameter, Darrieus vertical axis wind turbine (VAWT), see Fig. 14, is a variable speed turbine that has been operated at fixed speeds throughout its operating range of 28 to 38 rpm and in a true variable speed mode. The turbine is located near Bushland, Texas. Its blades are made from extruded aluminum. A typical cycle count distribution for the flatwise bending is shown with the generalized Weibull curve fit in Figures 15 and 16.

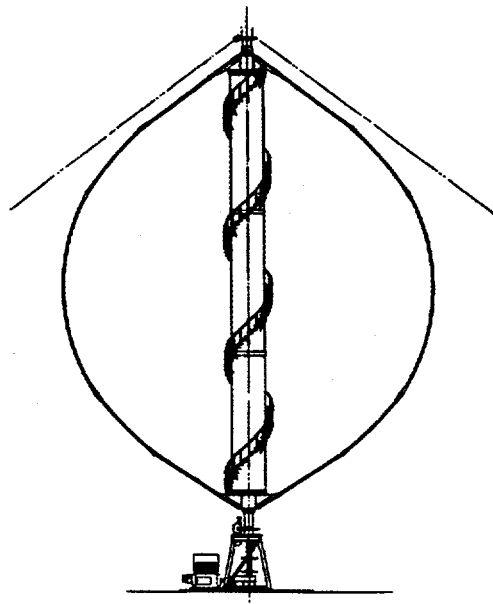


Fig. 14. The Sandia 34-m Test Bed Turbine.

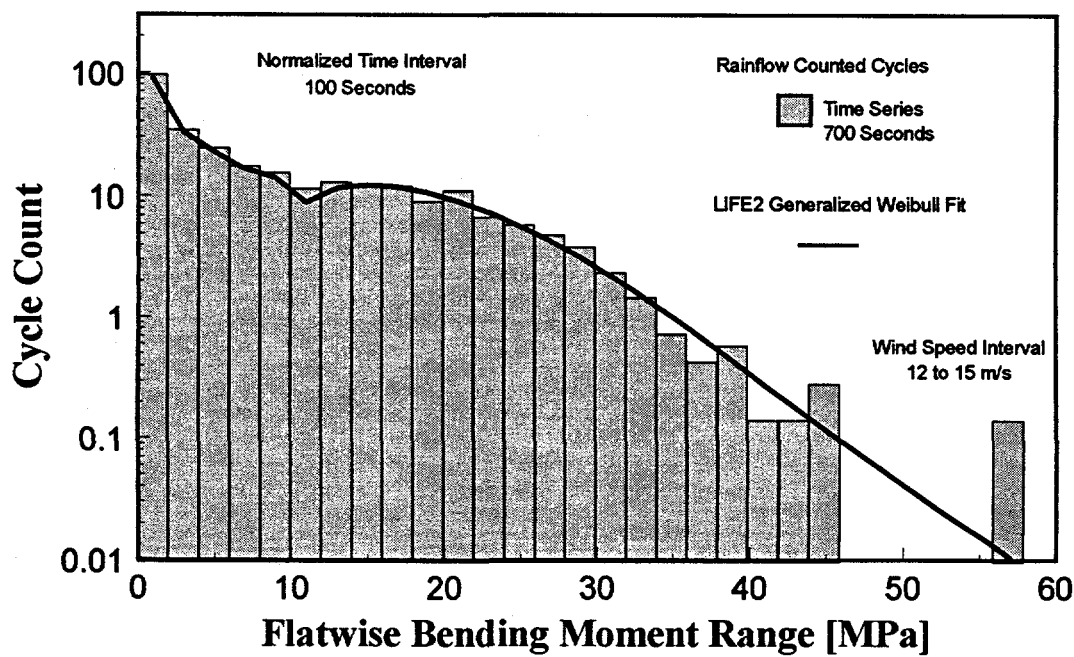


Figure 15. Comparison of Rainflow Counted Stress Cycles and the Generalized Weibull Fit for the Sandia 34-m VAWT.

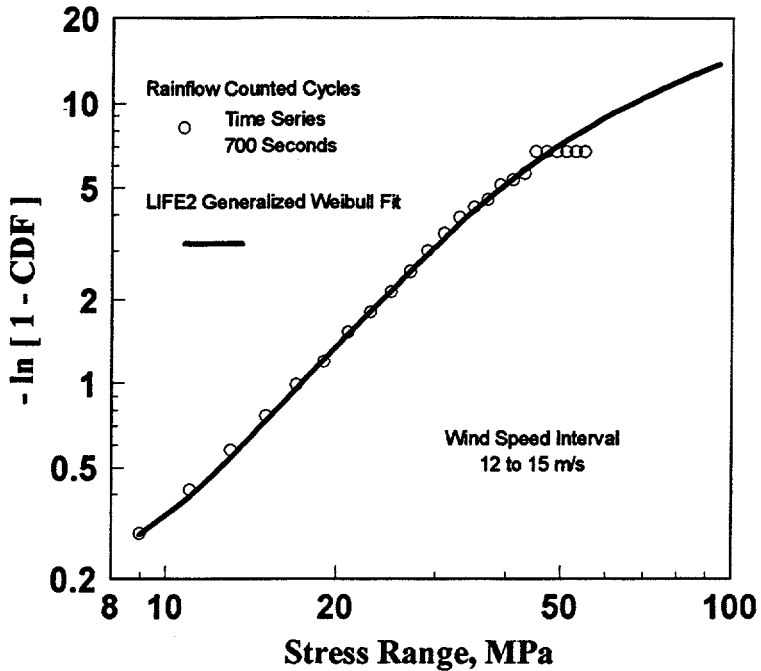


Figure 16. Generalized Weibull Plot of Rainflow Counted Stress Cycles and the Generalized Weibull Fit for the Sandia 34-m VAWT.

Sutherland and Veers [7] analyzed data records from the upper root of this turbine to predict the service lifetime. In their analysis, the operational stress states were determined using both time series data and frequency synthesized data. The frequency synthesis analyses are used here to evaluate the generalized fitting technique's ability to extrapolate the tail of a typical wind turbine cycle count distribution.

As noted by Sutherland and Veers [7], the frequency domain analysis permits the synthesis of very long time series data to fill the population of the stress distribution in the high-stress region; thus, the technique simulates the effect of having longer data samples. The histogram shown in Figures 17 and 18 compares the cycle counts from approximately 700 seconds of time data to the cycle counts obtained from over 2,700,000 seconds of synthesized time series data and the generalized Weibull fit to the 700 seconds of data. As shown in Figure 18, the curve fit to the 700 seconds of data diverges from the frequency synthesized data in the tail of the distribution, i.e., above a range of approximately 50. As the 700-second data block contains only a single count in this high range, the curve fit has extrapolated the body of the distribution beyond statistically significant data. The comparison to the 2,700,000 seconds of synthesized data indicates that the extrapolation contains too few cycle counts in the tail of the distribution. As noted by several authors [1, 3 and 7], the poor quality of the extrapolation is probably a result of the relatively short length of the rainflow-counted data block (i.e., the data does not contain a sufficient number of stress cycles in the tail of the distribution to be statistically significant). Thus, the extrapolation is consistent with the information contained in the short data block and should not be expected to be a replacement for more data.

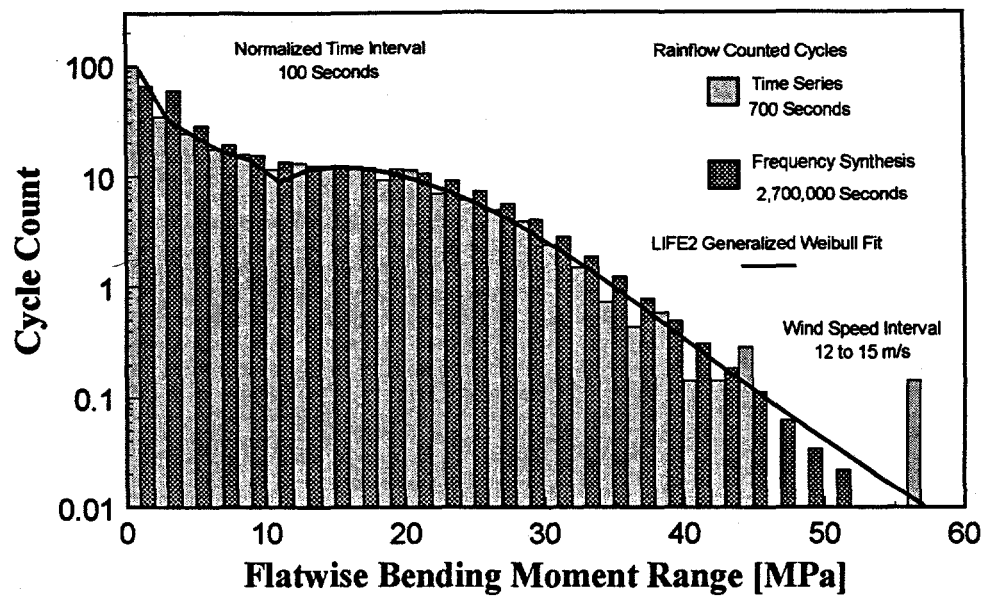


Figure 17. Comparison of the Frequency Synthesized Stress Cycle Distribution to the Rainflow Counted Stress Cycles and the Generalized Weibull Fit for the Sandia 34-m VAWT.

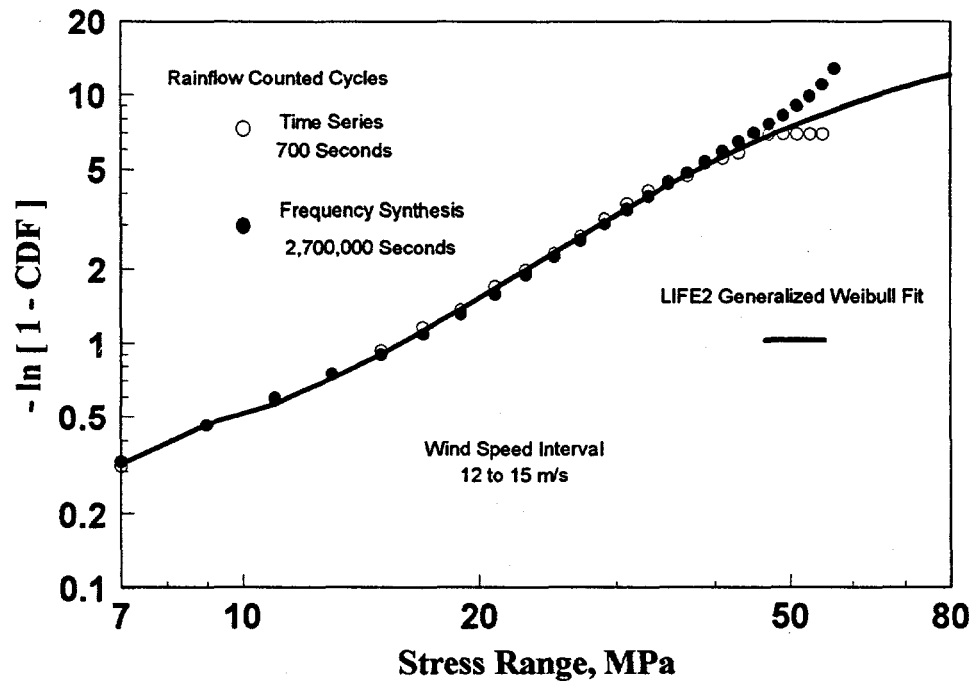


Figure 18. Generalized Weibull Plot of the Frequency Synthesized Stress Cycle Distribution to the Rainflow Counted Stress Cycles and the Generalized Weibull Fit for the Sandia 34-m VAWT.

To determine if the fitting routine would do better if additional data were available, the code was used to fit a 10,200 second data block that was obtained using frequency synthesis techniques. The comparison, shown in Figure 19, illustrates that the extrapolation from 10,200 seconds is significantly more consistent with the 2,700,000 seconds of data than it is with the extrapolation from 700 seconds of data.

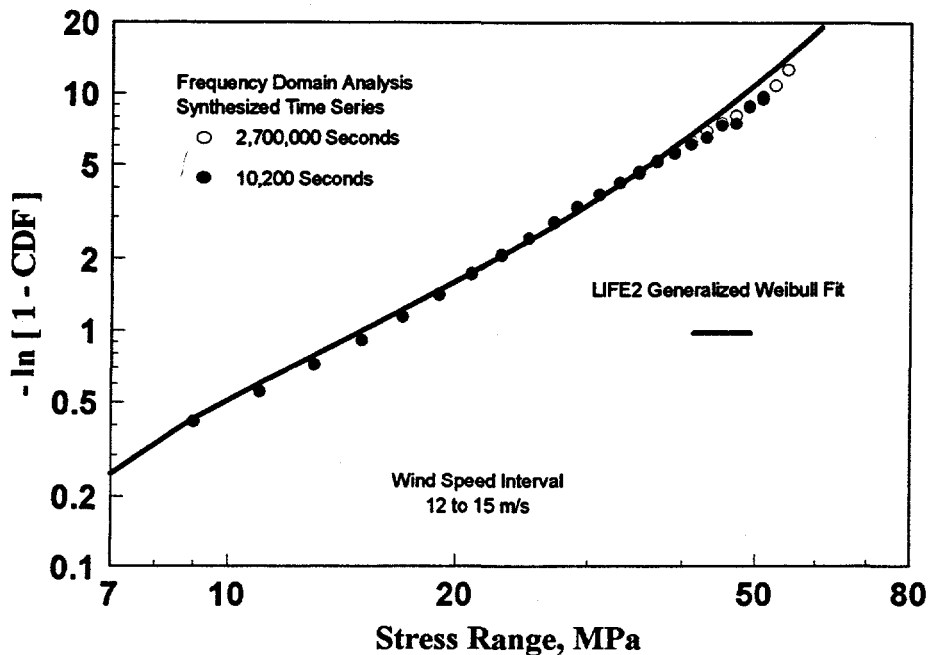


Figure 19. Generalized Weibull Plot of the Frequency Synthesized Stress Cycle Distributions for the Sandia 34-m VAWT.

CONCLUDING REMARKS

As demonstrated in the examples cited above and in Winterstein and Lange [1], the generalized Weibull technique can fit a variety of distributions of fatigue stress cycles for wind turbines. These fits are very good in the body of the distribution, where ample data is available, and permit an extrapolation to the tail of the distribution, where ample data are not available.

The generalized Weibull technique is an important tool in the fatigue analysis of wind turbines. This technique, with its pre- and post-processing algorithms, is now incorporated into the LIFE2 fatigue analysis code for wind turbines.

BIBLIOGRAPHY

1. Winterstein, S. R., and Lange, C. H., "Load Models for Fatigue Reliability from Limited Data," *Wind Energy-1995*, ASME, SED-Vol. 16, 1995, pp. 73-82.
2. Winterstein, S. R., C. H. Lange, and S. Kumar, *FITTING: A Subroutine to Fit Four Moment Probability Distributions to Data*, Rept. RMS-14, Rel. Marine Struc. Prog., Civil Eng. Dept., Stanford University, Stanford, CA, 1995.
3. H. J. Sutherland and C. P. Butterfield, "A Summary of the Workshop on Fatigue Life Methodologies for Wind Turbines," *Proceedings of WindPower '94*, AWEA, 1994, pp. 279-292.
4. Jackson, K. L., "Deriving Fatigue Design Loads from Field Test Data," *Wind Power '92*, AWEA, 1992, pp. 313-320.
5. Malcolm, D. J., "Predictions of Peak Fatigue Stresses in a Darrieus Rotor Wind Turbine Under Turbulent Winds," *Ninth ASME Wind Energy Symposium*, D. E. Berg (ed), SED-Vol. 9, ASME, 1990, pp. 125-135.
6. N. D. Kelley, "A Comparison of Measured Wind Park Load Histories with the WISPER and WISPERX Load Spectra," *Wind Energy - 1995*, (ed), SED-Vol. 16, ASME, 1995, pp. 107-114.
7. H. J. Sutherland and P. S. Veers, "Effects of Cyclic Stress Distribution Models on Fatigue Life Predictions," *Wind Energy - 1995*, (ed), SED-Vol. 16, ASME, 1995, pp. 83-90.
8. H. J. Sutherland and L. L. Schluter, "Fatigue Analysis of WECS Components Using a Rainflow Counting Algorithm," *Proceedings of Windpower '90*, AWEA, 1990, pp. 85-92.
9. Schluter, L. L., and Sutherland, H. J., *Reference Manual for the LIFE2 Computer Code*, SAND89-1396, Sandia National Laboratories, Albuquerque, NM, 1989.
10. Sutherland, H. J., *Analytical Framework for the LIFE2 Computer Code*, SAND89-1397, Sandia National Laboratories, Albuquerque, NM, 1989.
11. Coleman, C., and McNiff, B., *Final Report: Dynamic Response Testing of the Northwind 100 Wind Turbine*, Subcontractor Report, SERI Cooperative Research Agreement #DE-FC02-86CH10311, Solar Energy Research Institute, Golden, CO, 1989.
12. Schluter, L. L., and Sutherland, H. J., *User's Guide for LIFE2's Rainflow Counting Algorithm*, SAND90-2259, Sandia National Laboratories, Albuquerque, NM, 1991.
13. Schluter, L. L., *Programmers Guide for LIFE2's Rainflow Counting Algorithm*, SAND90-2259, Sandia National Laboratories, Albuquerque, NM, 1991.

14. Sutherland, H. J., and Linker, R. L., *User's Guide for the Frequency Domain Algorithms in the LIFE2 Fatigue Analysis Code*, SAND93-1900, Sandia National Laboratories, Albuquerque, NM, 1993.

APPENDIX A

EXAMPLE SESSION WITH TYPICAL RESULTS

This volume is the sixth in a series of Reference/User's Manuals for the LIFE2 code. The other 5 volumes are listed as References 9, 10, 12, 13 and 14. This section of the paper assumes that the reader has the other volumes available for reference.

Documenting Units

The LIFE2 code is unit insensitive. The user must assure that compatible units are used throughout the calculation. The code will ask for the units being used in the calculation so that they may be documented in the data files. As this module uses the rainflow algorithm already contained in the LIFE2 code, the output of the computational module will produce rainflow counts based on either the RANGE (peak-to-peak) or the AMPLITUDE (half range) of the stress cycle.

Operator Inputs

The following is an example session using the curve fitting algorithms that have been incorporated into the LIFE2 code. The data and fits for Northern Power edgewise data, cited above, will be used in this example.

In the example, LIFE2 code prompts are written in **bold** letters. The operator's responses to the prompts are written in *italics*.

Access

Starting at the Main Menu, the curve fitting routine is accessed via the Stress State Module. The current version of the LIFE2 code is 3.07.

LIFE2 -- Version 3.07

>>> Main Menu <<<

The options at this level are

- 1) Enter the Wind Spectrum**
- 2) Enter the Constitutive Properties**
- 3) Enter the Stress States**
- 4) Enter the Operational Parameters**
- 5) Calculate the Life of a WECS Component**

- 9) Exit Life2 Code**

Enter the number of the desired option.>3

Then, for any of the three classes of Stress States:

>>> Stress State Menu <<<

This menu allows the operator to select which type of stress matrix to input.

The options at this level are

- 1) Enter Operational Stresses**
- 2) Enter Buffeting Stresses**
- 3) Enter Start/Stop Stresses**

- 9) Return to Main Menu**

Enter the number of the desired option.>/

In this example, we will use the operational stresses for the edgewise bending stresses of the Northern Power turbine. The Buffeting and Start/Stop Stresses Menus are similar.

>>> Operational Stresses Menu <<<

This option allows the operator to input the operational stresses for a wind turbine.

The current Operational Stress Data Base in operational memory is NPS Data; Ch 3 - Root Edgewise Bending; 3Jun92

The stress units for this file are: MPa

The wind speed units for this file are: m/s

The options at this level are

- 1) Retrieve data from the Operational Stresses Library**
- 2) Input Tabular Operational Stress Data**
- 3) Calculate New Operational Stress Data**
- 4) Process Limited Time Data**
- 5) Plot an Operational Stress Data File**
- 6) Change Units of Wind Speed and/or Stress**
- 7) Add a Data File to the Operational Stresses Library**
- 8) Delete a Data File from the Operational Stresses Library**

- 9) Return to the Stress State Menu**

Enter the number of the desired option.>4

Curve Fitting from the Limited Time Data Menu

We chose to process the "Limited Time Data contained in the current operational stresses calculational file that is identified by its Header as " NPS Data; Ch 3 - Root Edgewise Bending; 3Jun92." The other reference manuals describe how to change this file to another and the other options in the Menu.

The options at this level are

- 1) Rainflow Count Time Series**
- 2) Rainflow Count from Frequency Spectra**
- 3) Curve Fit Limited Time Data**

9) Return to the Operational Stress Menu

Enter the number of the desired option.>3

Rainflow counting is covered in References 15 and 16. The analysis of spectral data is covered in Ref. 17. Here, we use the curve fitting algorithms by choosing option 3.

Is the data to be fitted in the current ops.cal file?

y

All "yes or no" answers may be answered by a simple y, Y, n or N. If the operator answer no to this query, the operator has another chance to change the current operational stresses calculational module.

The code then provides information about the data contained in the current operational stresses calculational module.

The total number of intervals: 1

1) Operational Stresses; # Records = 1; Range 9.00 to 11.00

Options:

F - Page Forward B - Page Backward
C - Curve Fit Interval E - Exit

Enter the desired option.>c

What is the interval number to be fitted?

I

In this case, the file contains one operational stress matrix. The header for this matrix indicates that they were obtained from 1 set of time series data (by rainflow counting) that was obtained under normal conditions with an average inflow speed of 9 to 11 m/s. These data are shown graphically in Fig. 2.

If the file contained more than 10 data sets, the "F and B" options could be used to examine the headers for all the data sets contained in the file. The "E" option takes the operator back to the previous menu. The "C" and the "1" options indicate that the operator wishes to curve fit interval 1.

When asked to fit a set of data, the code returns information concerning the data and asks for the lower limit of the curve fit. In this case, the alternating stress component of the fatigue cycles (amplitude or range) covers a range of 0.5 to 20.5 MPa, see Fig. 4. As noted above (see the section entitled "Lower Bound" on page 7), when a bi-modal distribution is being fit, the lower bound should be chosen to be near the beginning of the second mode, i.e., at approximately 8 MPa for this distribution.

The range covered is .50000 to 20.50000 MPa
Enter lower limit
8

The code then displays the RMS of the distribution, 1.17 MPa in this example. The operator then chooses the level to which the curve fit will be truncated (see the section entitled "Truncation" on page 8). In this case, the fit is truncated by the operator at 15 times the RMS or approximately 17.7 MPa above the chosen lower bound of 8 MPa. Thus, the fit is truncated at a maximum of 23.7 MPa (8 MPa + 17.7 MPa).

The current RMS value is 1.17838
The curve fit will be truncated at 10.00 times the RMS value.

Do you want to change this value (Y or N)?y

Truncate the distribution at what multiple of the RMS value?
(suggested value is 10.0)

15

The code then offers three classes of fits (see the section entitled "Parent Distribution" on page 7 and Refs. 1 and 2). The operator chooses the Weibull distribution here.

1: FIT GENERALIZED GAUSSIAN DISTRIBUTION
2: FIT GENERALIZED GUMBEL DISTRIBUTION
3: FIT GENERALIZED WEIBULL DISTRIBUTION

Enter type (1-3):

3

The operator then chooses the error tolerance to which the curve will be fit. In this case, a 1% value is chosen.

Enter error tolerance:

(.01 = 1%)

.01

For the case cited above, the curve fitting algorithm was able to fit the data with an error tolerance of 1percent. If the code had not been able obtain the desired error tolerance, it prints a message to the effect:

**. WARNING(OPT): THE OPTIMAL MODEL USED GIVES
AN ERROR OF .225816 IN THE NORM OF SKEWNESS AND
KURTOSIS.**

Press <enter> to continue.

<enter>

The code performs the curve fit to the selected interval, saves the fit in the operational stresses calculational file, updates the header for the interval that was fit, and returns the operator to the interval description menu. If other intervals are to be fit, the operator may proceed as described above. In this case, we have curve fit the single stress cycle matrix contained in the ops.cal file. With the "E" option, we conclude the curve fitting process for this file.

The total number of intervals: 1

1) Operational Stresses; # Records = 1; Range 9.00 to 11.00; CF

Options:

**F - Page Forward B - Page Backward
C - Curve Fit Interval E - Exit**

Enter the desired option.>e

Note that the header for this set of data has been modified with a "CF" designation to indicate to the operator that it has been curve fit.

The notes at the end of the operational stresses calculational file are then displayed and the operator may change them. In this case we will add one note.

The following notes currently exist for this file:

Operator: HJS

Start 3Jun92: 9 Channels of Info

The current options are

- 1) Leave the notes as they are**
- 2) Add new notes to the existing notes**
- 3) Delete old notes and add new notes**

Enter the number of the desired option.

2

Enter the number of additional notes.

1

Enter note 1; no longer than 72 characters.

Interval 1: Curve Fit using a Weibull Distribution. HJS

The notes are then updated and the operator is returned to the "Limited Time Data Menu." A series of 9's will return the operator to the main menu or to the DOS prompt.

The options at this level are

- 1) Rainflow Count Time Series**
- 2) Rainflow Count from Frequency Spectra**
- 3) Curve Fit Limited Time Data**

- 9) Return to the Operational Stress Menu**

Enter the number of the desired option.>9

APPENDIX B

PLOTTING THE RESULTS

To plot the data generated by this or any other stress state modules, return to the operational, buffeting, or start/stop stress state menu and choose option 5 from the "Operational Stresses Menu."

>>> Operational Stresses Menu <<<

This option allows the operator to input the operational stresses for a wind turbine.

**The current Operational Stress Data Base in operational memory is
NPS Data; Ch 3 - Root Edgewise Bending; 3Jun92**

The stress units for this file are: MPa

The wind speed units for this file are: m/s

The options at this level are

- 1) Retrieve data from the Operational Stresses Library**
- 2) Input Tabular Operational Stress Data**
- 3) Calculate New Operational Stress Data**
- 4) Process Limited Time Data**
- 5) Plot an Operational Stress Data File**
- 6) Change Units of Wind Speed and/or Stress**
- 7) Add a Data File to the Operational Stresses Library**
- 8) Delete a Data File from the Operational Stresses Library**

- 9) Return to the Stress State Menu**

Enter the number of the desired option.>5

We wish to plot the current calculational stresses data contained in the ops.cal file.

The total number of intervals: 1

1) Operational Stresses; # Records = 1; Range 9.00 to 11.00; CF

Options:

F - Page Forward B - Page Backward
P - Plot Interval E - Exit

Enter the desired option.>p

What is the interval number to be plotted?

I

If the stress plotting parameter have not been set previously, the operator will be asked a set of questions to determine these parameters. If they have been set previously, the parameters are retained by the code and used for the current plot. The code first queries the operator about the type of plot desired.

>>>Stress Plotting Menu<<<

The options at this level are:

- 1) Change Plot Parameters**
- 2) 2d-Plot of Alternating Stresses**
- 3) 2d-Plot of Mean Stresses**
- 4) 3d-Plot of Mean and Alternating Stresses**

- 9) Return to Operational Stresses Menu**

Enter the number of the desired option.>4

In this case, the operator choose a 3-D plot of the results. The operator is then queried about the type of scale to use.

Would you like the plot to be semi-logarithmic? (Y/N)

y

.....Plotting

**READY TO DISPLAY DRAWING.
Press <return> when ready to continue.**

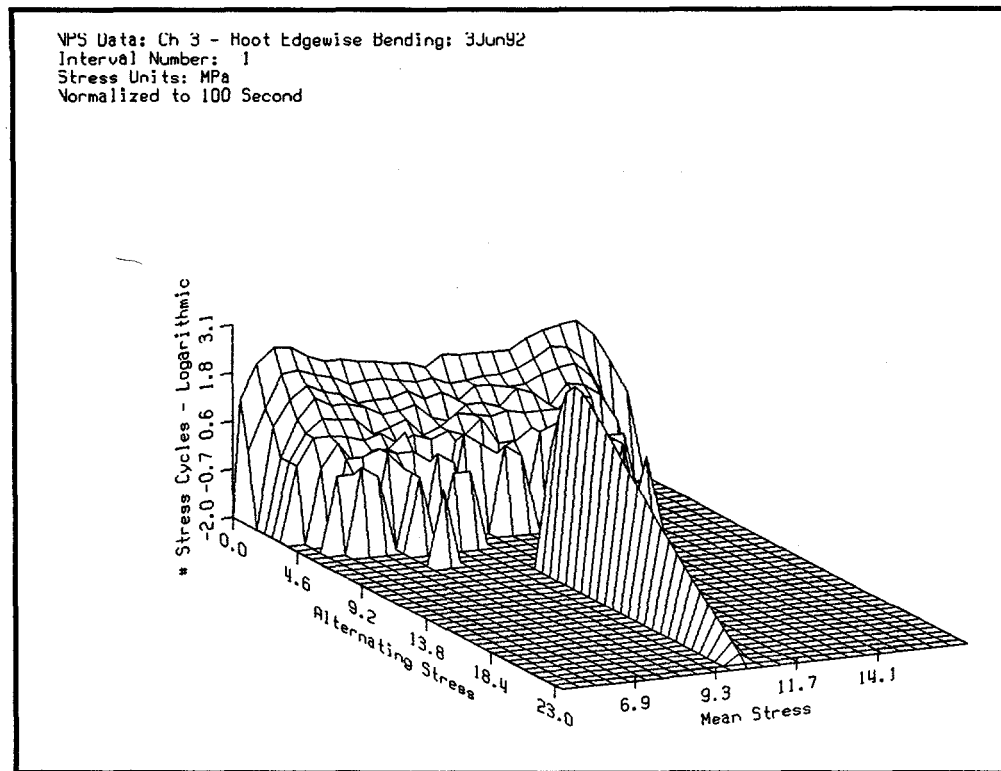


Fig. 20. Screen Display of the Generalized Weibull Fit of the 9 to 11 m/s Interval in the Operational Stresses Calculational File.

The computer completes the calculations required to make the plot and notifies the operator it is ready to complete the plot. When the operator depresses the "enter" button, the plot is produced, see Fig. 20.

The operator is then given the option to print a hard copy of the plot and to create a "cgm" formatted file of the plot.

Would you like a hard copy of the plot? (Y/N)

y

.....Plotting

Would you like to create a Computer Graphics Metafile (3d_plot.cgm)? (Y/N)

y

The operator is then returned to the "Stress Plotting Menu" to create additional plots or to use 9 to return to the main menu or to the DOS prompt.

>>>Stress Plotting Menu<<<

The options at this level are:

- 1) Change Plot Parameters**
- 2) 2d-Plot of Alternating Stresses**
- 3) 2d-Plot of Mean Stresses**
- 4) 3d-Plot of Mean and Alternating Stresses**

- 9) Return to Operational Stresses Menu**

Enter the number of the desired option.>9

DISTRIBUTION

R. E. Akins
Washington & Lee University
P.O. Box 735
Lexington, VA 24450

H. Ashley
Dept. of Aeronautics and
Astronautics Mechanical Engr.
Stanford University
Stanford, CA 94305

Hui Bau
NSE Composites Stress Services
6417 Woodland Place North
Seattle, WA 98103

B. Bell
FloWind Corporation
990 A Street
Suite 300
San Rafael, CA 94901

K. Bergey
University of Oklahoma
Aero Engineering Department
Norman, OK 73069

B. Boursier
Kenetech
6952 Preston Ave.
Livermore, CA 94550

C. P. Butterfield
NREL
1617 Cole Boulevard
Golden, CO 80401

G. Bywaters
New World Power Technology Center
Box 999
Waitsfield, VT 05673

J. Cadogan
U.S. Department of Energy
Office of Photovoltaic & Wind
Technology
Energy Efficiency & Renewable Energy
EE-11
1000 Independence Avenue SW
Washington, DC 20585

S. Calvert
U.S. Department of Energy
Office of Photovoltaic & Wind
Technology
Energy Efficiency & Renewable Energy
EE-11
1000 Independence Avenue SW
Washington, DC 20585

J. Chapman
OEM Development Corp.
840 Summer St.
Boston, MA 02217-1533

R. N. Clark
USDA
Agricultural Research Service
P.O. Drawer 10
Bushland, TX 79012

J. Cohen
Princeton Economic Research, Inc.
1700 Rockville Pike
Suite 550
Rockville, MD 20852

C. Coleman
Northern Power Systems
Box 659
Moretown, VT 05660

R. Davis
Convergence Engineering Co.
5056 Sunrise Blvd., Suite B3
Fair Oaks, CA 95628

K. J. Deering
The Wind Turbine Company
515 116th Avenue NE
No. 263
Bellevue, WA 98004

E. A. DeMeo
Electric Power Research Institute
3412 Hillview Avenue
Palo Alto, CA 94304

A. J. Eggers, Jr.
RANN, Inc.
260 Sheridan Ave., Suite 414
Palo Alto, CA 94306

D. M. Eggleston
DME Engineering
P.O. Box 5907
Midland, TX 79704-5907

P. R. Goldman
Acting Deputy Director
Office of Photovoltaic and
Wind Technology
Energy Efficiency & Renewable
Energy, EE-11
U.S. Department of Energy
1000 Independence Avenue
Washington, DC 20585

G. Gregorek
Aeronautical & Astronautical Dept.
Ohio State University
2300 West Case Road
Columbus, OH 43220

C. Hansen
University of Utah
Department of Mechanical Engineering
Salt Lake City, UT 84112

L. Helling
Librarian
National Atomic Museum
Albuquerque, NM 87185

S. Hock
Wind Energy Program
NREL
1617 Cole Boulevard
Golden, CO 80401

M. A. Ilyan
Pacific Gas and Electric Co.
3400 Crow Canyon Road
San Ramon, CA 94583

B. J. Im
McGillim Research
4903 Wagonwheel Way
El Sobrante, CA 94803

K. Jackson
Dynamic Design
123 C Street
Davis, CA 95616

G. James
University of Houston
Dept. of Mechanical Engineering
4800 Calhoun
Houston, TX 77204-4792

O. Krauss
Division of Engineering Research
Michigan State University
East Lansing, MI 48825

C. Lange
Civil Engineering Dept.
Stanford University
Stanford, CA 94305

R. Lynette
AWT/RLA
425 Pontius Avenue North
Suite 150
Seattle, WA 98109

D. Malcolm
Advanced Wind Turbines, Inc.
425 Pontius Avenue North
Suite 150
Seattle, WA 98109

J. F. Mandell
Montana State University
302 Cableigh Hall
Bozeman, MT 59717

T. McCoy
R. Lynette & Associates, Inc.
15042 N.E. 40th Street
Suite 206
Richmond, WA 98052

R. N. Meroney
Dept. of Civil Engineering
Colorado State University
Fort Collins, CO 80521

P. Migliore
NREL
1617 Cole Boulevard
Golden, CO 80401

A. Mikhail
Zond Systems, Inc.
13000 Jameson Road
P.O. Box 1910
Tehachapi, CA 93561

S. Miller
2321 Osprey Lane
Richland, WA 99352-9182

W. Musial
NREL
1617 Cole Boulevard
Golden, CO 80401

NWTC Library
NREL
1617 Cole Boulevard
Golden, CO 80401

V. Nelson
Department of Physics
West Texas State University
P.O. Box 248
Canyon, TX 79016

G. Nix
NREL
1617 Cole Boulevard
Golden, CO 80401

J. W. Oler
Mechanical Engineering Dept.
Texas Tech University
P.O. Box 4289
Lubbock, TX 79409

R. Osgood
NREL
1617 Cole Boulevard
Golden, CO 80401

R. G. Rajagopalan
Aerospace Engineering Department
Iowa State University
404 Town Engineering Bldg.
Ames, IA 50011

D. Sanchez
U.S. Dept. of Energy
Albuquerque Operations Office
P.O. Box 5400
Albuquerque, NM 87185

L. Schienbein
CWT Technologies, Inc.
4006 S. Morain Loop
Kennewick, WA 99337

K. Starcher
AEI
West Texas State University
P.O. Box 248
Canyon, TX 79016

F. S. Stoddard
Dynamic Design-Atlantic Office
P.O. Box 1373
Amherst, MA 01004

A. Swift
University of Texas at El Paso
320 Kent Ave.
El Paso, TX 79922

W. V. Thompson
410 Ericwood Court
Manteca, CA 95336

R. W. Thresher
NREL
1617 Cole Boulevard
Golden, CO 80401

W. A. Vachon
W. A. Vachon & Associates
P.O. Box 149
Manchester, MA 01944

B. Vick
USDA, Agricultural Research Service
P.O. Drawer 10
Bushland, TX 79012

L. Wendell
2728 Enterprise Dr.
Richland, WA 99352

R. E. Wilson
Mechanical Engineering Dept.
Oregon State University
Corvallis, OR 97331

S. R. Winterstein
Civil Engineering Department
Stanford University
Stanford, CA 94305

M. Zuteck
MDZ Consulting
931 Grove Street
Kemah, TX 77565

M.S. 0167 C. Miller, 12621
M.S. 0437 E. D. Reedy, 9118
M.S. 0437 K. E. Metzinger, 9118
M.S. 0439 C. R. Dohrmann, 9234
M.S. 0439 D. W. Lobitz, 9234
M.S. 0439 D. R. Martinez, 9234
M.S. 0443 J. G. Arguello, 9117
M.S. 0443 H. S. Morgan, 9117
M.S. 0555 B. Hansche, 9742
M.S. 0557 T. J. Baca, 9741
M.S. 0557 T. G. Carne, 9741
M.S. 0557 J. P. Lauffer, 9741
M.S. 0615 A. Beattie, 9742
M.S. 0615 W. Shurtleff, 9752
M.S. 0708 H. M. Dodd, 6214 (50)
M.S. 0708 T. D. Ashwill, 6214
M.S. 0708 D. E. Berg, 6214
M.S. 0708 M. A. Rumsey, 6214
M.S. 0708 H. J. Sutherland, 6214 (10)
M.S. 0708 P. S. Veers, 6214
M.S. 0708 T. A. Wilson, 6214 (5)
M.S. 0836 J. H. Strickland, 9116
M.S. 0836 G. F. Homicz, 9116
M.S. 0836 W. Wolfe, 9116
M.S. 0958 T. R. Guess, 1472
M.S. 0619 Review & Approval Desk,
12630 (2) For DOE/OSTI
M.S. 0899 Technical Library, 4414 (5)
M.S. 9018 Central Technical Files, 8523-2